

Research Article

Open Access, Volume 5

Native and modified starch nano-crystals loaded with doxorubicin mediated apoptosis in human breast cancer MCF7 cells**Oluyemisi A Bamiro^{1,2}; Lunawati L Bennett^{2*}; and Michael A Odeniyi³**¹Department of Pharmaceutics & Pharmaceutical Technology, Faculty of Pharmacy, Olabisi Onabanjo University, Nigeria.²College of Pharmacy, Union University, Jackson, TN, USA.³Department of Pharmaceutics & Industrial Pharmacy, Faculty of Pharmacy, University of Ibadan, Nigeria.***Corresponding Author: Lunawati L Bennett**1050 Union University Drive, Union University,
College of Pharmacy, Jackson, TN 38305, USA.

Email: llbennett@uu.edu

Received: Feb 20, 2024

Accepted: Mar 07, 2024

Published: Mar 14, 2024

Archived: www.jcimcr.org

Copyright: © Bennett LL (2024).

DOI: www.doi.org/10.52768/2766-7820/2921

Abstract

The present study was aimed at evaluating the effect of doxorubicin (Dox) loaded nanocrystals starch in human breast cancer MCF7 cells. A model for breast cancer, MCF7 cells, were treated with Dox loaded in S (native starch), NS (starch nanocrystal), ANS (acetylated starch nanocrystal) extracted from *Oryza glaberrima* Steud and compared with Dox (diluted in water). MTT assay, Hoechst33342, H2DCFDA, Live Death, and Rhodamine123 staining, and Western Blot were used to detect different signaling protein expressions and apoptosis. Hoechst33342 staining showed cellular apoptosis of MCF7 after treating with DOX loaded S, NS, ANS or Dox alone. Intracellular ROS levels, p53 and Bax/Bcl2 expressions, and decrease in mitochondrial membrane potential were also higher in MCF7 cells treated with Dox loaded S, NS, ANS or Dox alone. To ensure Dox loaded S, NS or ANS did not cause any cellular damages to normal cells, HEK-293 kidney cells were used as control. Dox loaded S, NS, or ANS were as effective formulations as Dox alone to decrease progression and metastasis of breast cancer in MCF7 cells. This study provides a novel approach for further investigation since Dox loaded starch nanocrystals are effective and can prevent side effects of cardiotoxicity when using Dox alone.

Keywords: Doxorubicin; Breast Cancer; Nanocrystals; *Oryza* Starch; MCF7.**Abbreviations:** ANS: Acetylated Starch Nanocrystal; Casp: Caspases; Cdk: Cyclin-Dependent Kinases; cl: Cleaved; DLC: Drug loading capacity; Dox: Doxorubicin; EGFR: Epidermal Growth Factor Receptor; FBS: Fetal Bovine Serum; H2DCFDA: 2', 7'-Dichlorodihydrofluorescein Diacetate; HEK-293: Human Embryonic Kidney Cells; LE: Loading Efficiency; MCF7: Human Breast Cancer Cells; MMP: Matrix Metallo Proteinase; MTT: 4, 5-dimethylthiazol-2-yl] -2, 5-diphenyl-tetrazolium bromide; NS: Starch Nanocrystal; PARP: Poly Adenosine Di-Phosphate Ribose Polymerase; P13K: Phosphatidylinositol-3 Kinase; ROS: Reactive Oxygen Species; S: Native Starch.

Introduction

The incidence of breast cancer mortality is one of the major health challenges and is complicated by drug resistance and toxicity of the drugs [1]. Doxorubicin is one of the most effective anti-cancer agents that have been used successfully to treat a variety of cancers including cancer of the blood, carcinoma, sarcoma and breast cancer. Doxorubicin belongs to anthracyclines antibiotic that exert its anti-cancer properties through several mechanisms of action. These mechanisms include intercalation into DNA, which directly affects transcription and replication, and inhibition of topoisomerase II activity by stabilizing the DNA topoisomerase II alpha complex preventing the ligation reaction. Further, it stabilizes the generation of free radicals as it cycles between its quinone and semi-quinone structures during metabolic reactions [2,5]. Although doxorubicin has been used in the treatment of many cancers, it causes cardiotoxicities showing as congestive heart failure or dilative cardiomyopathy after a single dose as early as 24 hours after exposure or many years later after successful treatment [6,7]. Because doxorubicin effectively treats a wide variety of cancers and patients' quality of life is improved when doxorubicin is included in the treatment regimen, significant efforts are being directed to formulate doxorubicin to make this drug less toxic, while still having the same efficacy like its natural formulation [3,8]. Native and modified starches have been widely used as biodegradable polysaccharides in drug delivery and tissue engineering [9,10]. Native starches (S) easily swell and degrade enzymatically, thus preventing them from being used in controlled drug delivery [11]. Modifications of starches using different methods such as acetylation can contribute to better controlled drug release [12]. The aim of the present study was to evaluate the chemo-enhancing potential of S, NS, and ANS loaded with doxorubicin in MCF7 cancer cell. Inhibition of cancer-signaling related pathways would be an evidence of the efficacy of the formulated starch on MCF7 cells.

Materials and methods

Materials: Doxorubicin, MTT (4, 5-dimethylthiazol-2-yl) -2, 5-diphenyl-tetrazolium bromide), RIPA buffer (50mM Tris-HCl, pH 8.0, 1% NP-40, 0.5% sodium deoxycholate, 150 mM NaCl, and 0.1% sodium dodecyl sulfate) protease and phosphatase inhibitors were purchased from Sigma (Saint Louis, MO, USA). Sorafenib base was purchased from LC Laboratories (Woburn, MA). Dimethyl sulfoxide (DMSO) was purchased from Amresco (Solon, OH, USA). NucBlue™ live cell stain (Hoechst33342 special formulation) was purchased from Life Technologies (Carlsbad, CA, USA), H2DCFDA (2', 7'-Dichlorodihydrofluorescein diacetate) was obtained from Invitrogen (Eugene, OR, USA), Rhodamine 123 was obtained from Thermo Fischer (Waltham, MA, USA), Nuclear-ID Red/Green cell viability reagent was purchased from Enzo Life science (Farmingdale, New York, USA). Bradford Reagent was supplied by Bio-Rad (Hercules, CA, USA). Primary antibodies Poly (ADP-Ribose) polymerase (PARP), casp-3, casp-9, p53, MMP2, and AKT were purchased from Cell Signaling Technology (Beverly, MA, USA), while Bax, Bcl2, Apaf-1, EGFR and β -actin were purchased from Santa Cruz Biotechnology, Inc (Santa Cruz, CA, USA). Secondary antibodies for anti-rabbit or anti-mouse were purchased from Cell Signaling Technology (Beverly, MA, USA).

Cell culture: The human breast cancer (MCF7) and human embryonic kidney (HEK-293) were purchased from ATCC (Manassas, VA, USA), cultured in DMEM media (Corning Cellgro, VWR Radnor, PA) supplemented with 10% fetal bovine serum (FBS) from ATCC, 1% streptomycin/penicillin from ATCC, and 0.1 % human insulin solution only for MCF7 (Santa Cruz Biotechnology, Inc, CA, USA). The cells were maintained in incubator at 37°C in 5% CO₂ humidified environment. Cell culture dishes (T75) were purchased from Greiner-Bio One (Monroe, NC, USA).

Preparation of rice starch nanocrystals: Native rice known as ofada rice (*Oryza glaberrima*) was purchased from Bodija Market, Ibadan, Nigeria and the starch extracted from the grains in the Pharmaceuticals Laboratory of University of Ibadan, Nigeria. The native starch (S) was extracted, the starch nanocrystals (NS) and acetylated starch nanocrystals (ASN) were prepared as described by Bamiro et al. [13].

Drug loading: 150 mg of the different starch samples were suspended in 10 mL of 1.0 mg/mL drug (doxorubicin) solution in distilled water and then incubated for 1 hour. The suspensions were centrifuged and washed with distilled water. The amount of drug in the supernatant was assayed using UV-visible Spectrophotometer according to the standard curves of the drug absorbance to concentration were determined as previously described [13].

Cytotoxicity assay: MCF7 and HEK-293 cells viabilities were assessed by MTT method as previously described [14,15]. Briefly, cells were plated in a 96-well, flat-bottomed microplate (Greiner-Bio One, Monroe, NC, USA) at a volume of 100 μ l per well (1×10^5 cells/ml) and incubated overnight in growth medium to allow the cells to adhere to the wells. The media was replaced with fresh media the next day. The cells were treated with serial concentrations of Dox loaded in NS, ANS, S or Dox alone. The treated cells were then incubated for 24 h in 5% CO₂ at 37°C. After 24 h incubation, 50 μ l MTT solution (2 mg/ml) was added to each well. Four hours after the incubation in 5% CO₂ at 37°C, media from each well was removed followed by addition of 150 μ l DMSO to dissolve violet blue crystals. The cytotoxicity of the drugs was determined by measuring the absorbance at 570 nm using spectrophotometer (Molecular Devices, CA, USA).

Analysis of apoptosis activation: Morphological changes of the nuclear chromatin inducing apoptosis were detected using Hoechst 33342 staining (NucBlue™ Live Cell Stain) as previously described [14,15]. Briefly, MCF7 cells seeded in 6 well plates were treated with Dox loaded in S, NS, or ANS, or Dox alone following incubation of cells for 24 h in 5% CO₂ at 37°C. The cells were stained according to the manufacturer's protocol. Stained cells were observed using FLoid cell imaging station (Life Technologies, Carlsbad, CA, USA) to assess the cellular apoptosis. A histogram was prepared to compare the percentage changes of apoptotic cells from different treatment groups using Image J software (NIH, USA).

Analysis of intracellular ROS generation: Intracellular ROS generation after treatment of cells was detected with H2DCF-DA in combination with Hoechst33342 as fluorescent probes as previously described [14,15]. Cells were treated with Dox loaded in S, NS, ANS or Dox alone incubated for 24 h at 5% CO₂ 37°C prior to addition of 20 μ M of H2DCF-DA and Hoechst

using protocol from the manufacturer. After 30 minutes, cells were washed with DPBS. The relative intensities of green fluorescence in different treated groups were captured using Floid cell imaging station under equivalent conditions. Fluorescence intensities were measured by Image J software and a histogram was prepared to compare relative fluorescence intensities in different treatment groups.

Analysis for mitochondrial membrane potential: Mitochondrial membrane potential in treated group was detected with Rhodamine 123 fluorescent probe method as previously described [14,15]. Briefly, MCF7 cells were plated in 6 well plates for 24 h and then treated with Dox loaded in NS, S, ANS or Dox alone in 5% CO₂ at 37°C for another 24 h prior to addition of 10 mM of Rhodamine123 according to the manufacturer's protocol. After 30 minutes, cells were washed with DPBS. The relative intensities of green fluorescence in different treated groups were captured using FLOID cell imaging station under equivalent conditions. Fluorescence intensities were measured with Image J software and a histogram was prepared to compare relative fluorescence intensities in different treatment groups.

Analysis of live and dead cells: The analysis of proportion of live and death cells was performed using Nuclear-ID Red/Green as fluorescent probe as previously mentioned [15]. Briefly, MCF7 cells were treated with Dox loaded in S, NS, ANS or Dox alone. After treatment, the MCF7 cells were incubated for 24 h in 5% CO₂ at 37°C, 2 µl of Nuclear-ID Red/Green was added using the manufacturer's protocol. The number of live cells showing as bright red color and dead cells as green cells were numbered with Image J software and a histogram was prepared to compare relative live and dead cells ratio from different treatment groups.

Expression of apoptotic pathway related proteins by Western blot analysis: The expressions of apoptotic signaling proteins were analyzed by Western blot technique as previously described [14,15]. Briefly, MCF7 or HEK-293 cells were treated with Dox loaded in S, NS, or ANS, or Dox alone. The cells were then washed with DPBS twice and the proteins were extracted in RIPA buffer with protease and phosphatase inhibitor cocktail. To separate proteins from cell debris, cells were centrifuged at 12,000 rpm for 30 minutes at 4°C. The protein concentrations were determined using the Bradford Protein Assay Reagent. Equivalent amounts of protein from each sample were loaded onto polyacrylamide gels and separated by electrophoresis using PowerPac200 electrophoresis system (BioRad Laboratories, Hercules, USA). The proteins were then transferred to Immuno-Blot PVDF membranes (BioRad Laboratories). Blotting was performed using TransBlot Turbo (BioRad Laboratories) for 30 minutes. The membranes were then blocked for 2 hours at room temperature in Tris-buffered saline with 0.1% Tween-20 (TBST) and 5% blotto. After washing, the membranes were incubated and rocked on a multi shaker overnight at 4°C with different primary antibodies of interest diluted in 3% TBST. The membranes were probed with horseradish peroxidase-conjugated anti-mouse IgG or anti-rabbit IgG antibody for 2 hours at room temperature. The protein band was developed by ECL Western Blotting detection reagents (BioRad Laboratories) and the pictures were taken using BioRad ChemiDoc XRS+ (BioRad Laboratories).

Statistical analysis: All data were expressed as the mean ± SD of three independent sets of experiments. Differences between individual and combination treatment groups were analyzed using Newman-Keuls one-way ANOVA.

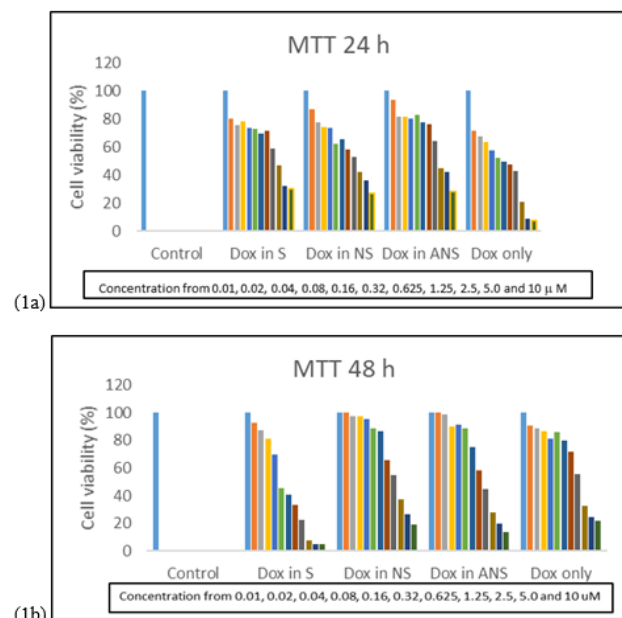


Figure 1: (a) MTT assay for cell viability of MCF7 cells after 24 h. MCF7 cells treated with different concentration of Dox loaded in S, NS, ANS or Dox alone ranging from 0 – 10 µM. (b) MTT assay with similar condition after 48 h. * P < 0.05, ** P < 0.01 and *** P < 0.001 were considered statistically significant.

Results

Physicochemical properties of Oryza glaberrima starch and starch nanocrystals: The density, solubility, swelling capacity, and hydration capacity of the starch increased after its modification. They formed aggregation with size ranged from 5-15 µm and the shape were polyhedrals. Chemical modification led to increase drug loading capacity (DLC) and loading efficiency (LE) of doxorubicin in the starch samples as previously reported [13].

MCF7 cell viability and selection of doses: Treatment of MCF7 cells for 24 h with Dox load in S, NS, ANS or Dox alone decreased cells viability in a dose dependent manner. Figure 1a and 1b showed that serial dilution of Dox loaded S, NS, ANS or Dox alone ranging from 0.01 µM to 10 µM cause decreased in cell viability from 5% to 95% after 24 h or 48 h of treatments. There was an initial decreased cell viability with DOX alone after 24 hours, but by 48 hours, the ranking of decreased cell viability was DOX-S > DOX-ANS > DOX-NS > DOX-alone

Table 1: IC₅₀ of Dox loaded in S, NS, ANS or Dox alone in HEK-293 kidney cells or in MCF7 breast cancer cells after 24 h or 48 hr.

	HEK-293-24 h	MCF7-24 h	HEK-293-48 h	MCF7- 48 h
Dox load in S	6.22	4.40	3.46	4.02
Dox load in NS	7.54	3.96	2.58	4.31
Dox load in ANS	9.62	4.97	3.36	4.60
Dox alone	4.15	1.50	0.84	1.58

IC₅₀ of Dox loaded NS, S, ANS in MCF7 and HEK-293: To compare cytotoxicity effect of Dox loaded in S, NS, ANS or Dox alone, MTT assay were also performed with same condition in HEK-293 kidney cells. Table 1 showed IC₅₀ of Dox loaded in S, NS, ANS or Dox alone. Dox alone has lower IC₅₀ than Dox loaded in S, NS, or ANS preparation (1.5 versus 4.4, 3.96, 4.97, respectively). Moreover, after 48 h treatment of cells with Dox loaded

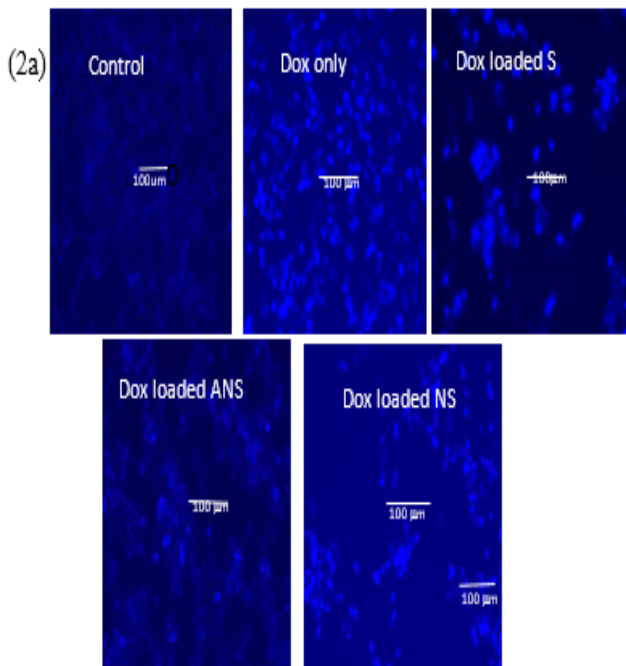


Figure 2a: Fluorescence microscopic images of apoptotic cells stained with Hoechst333342. The number of apoptotic cells (bright nuclei) was increased in Dox loaded S, NS or ANS, with the highest number of apoptotic cells was noticed in MCF7 cells treated with Dox alone as compared to control. Scale bar indicates 100 μm .

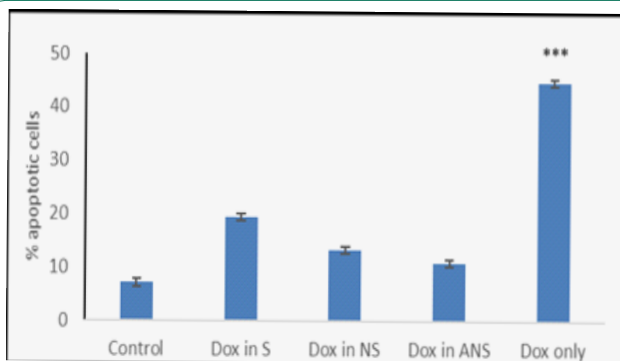


Figure 2b: Histogram represents the percentage of apoptotic cells from the different treatment groups vs. control MCF7 cells (**=0.01<p, ***=0.001<p).

in S, NS, ANS or Dox alone, there was no significant difference in their IC50. Treatment of HEK-293 kidney cells with Dox loaded in S, NS, or ANS preparation showed higher IC50 than in MCF7 breast cancer cells (6.22 vs. 4.40; 7.54 vs. 3.96; 9.62 vs. 4.97; and 4.15 vs. 1.50), respectively. This data showed Dox loaded in S, NS, ANS can be used to treat cancer cells (i.e. breast cancer MCF cell) without causing cytotoxicity effect to the normal cells (i.e. HEK-293 kidney cells).

Doxorubicin loaded S, NS, ANS, or Dox alone induce apoptosis: The extent of apoptosis induced by Dox loaded in S, NS, ANS, or Dox alone in MCF7 cells was confirmed by Hoechst33342 staining and detected using fluorescence microscopic images. Figure 2a demonstrated that the nucleus of control MCF7 cells showed lower fluorescence intensity signifying that these cells were normal and healthy. The cells undergoing apoptosis, showed brightly stained nucleus due to condensed and fragmented nucleus. In Dox loaded S, NS, ANS, or Dox alone, the percentage of brightly stained cells was higher than control. Figure 2b showed histogram of the percentage of apoptotic cells from control MCF7 and MCF cells treated with Dox loaded S, NS, ANS, or Dox alone.

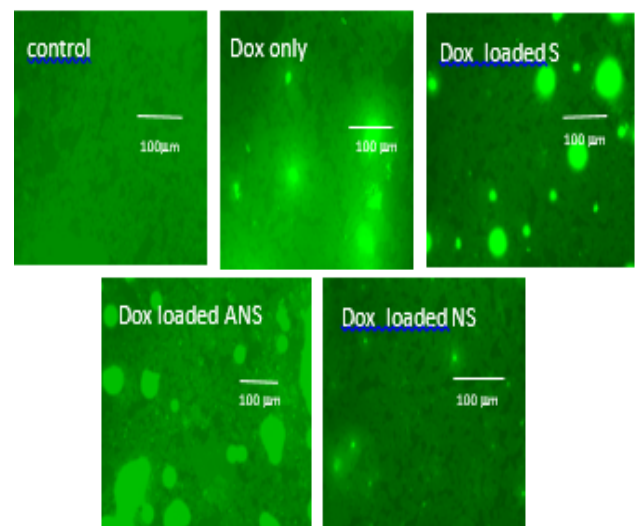


Figure 3: Fluorescence microscopic images of intracellular reactive oxygen species (ROS) generation in MCF7 cells after 24 h treatment with Dox loaded S, NS, ANS or Dox alone. After H2DCFDA staining, there was no changes in cell fluorescence, i.e. ROS was observed in the MCF7 control, however significant higher levels of ROS were observed in MCF7 cells treated with Dox loaded S, NS, or ANS. Scale bar indicates 100 μm .

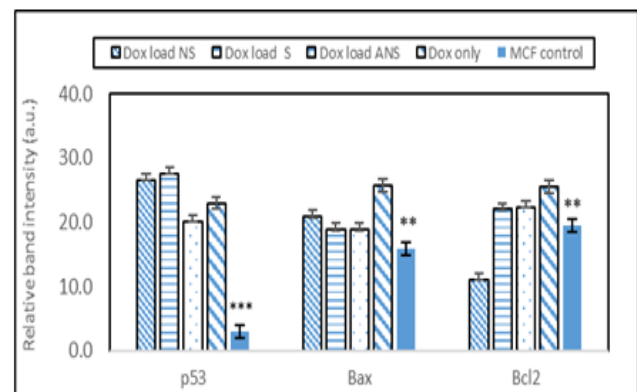
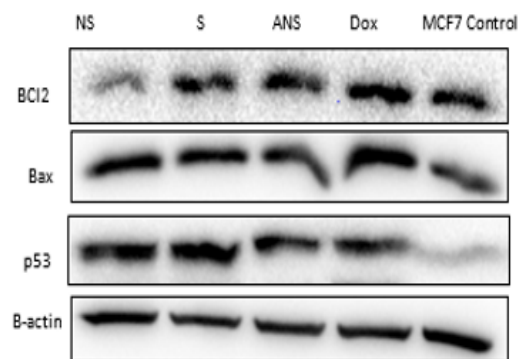


Figure 4: (a) Western blot analysis data in MCF7 for the modulation expression of p53, Bax, Bcl2 proteins after treatment with Dox loaded S, NS, ANS or Dox alone. p53 and Bax expression was significantly higher than control (**=0.01 < p, ***=0.001 < p). Higher level of p53 was observed in Dox loaded S, NS, or ANS than Dox alone. **(b)** Histogram bar intensity from the modulation of the p53, Bax, and Bcl2 proteins in MCF7 cells.

Doxorubicin loaded S, NS, ANS, or Dox alone caused intracellular ROS: Generation of intracellular ROS after treatment of MCF7 cells with Dox loaded in S, NS, ANS, or Dox alone was evaluated by H2DCFDA staining. Figure 3 showed the difference in fluorescence intensity levels using the fluorescence microscopic images. These photomicrographs showed that the cells had higher H2DCFDA fluorescence intensity than control cells as shown in bright green dyes.

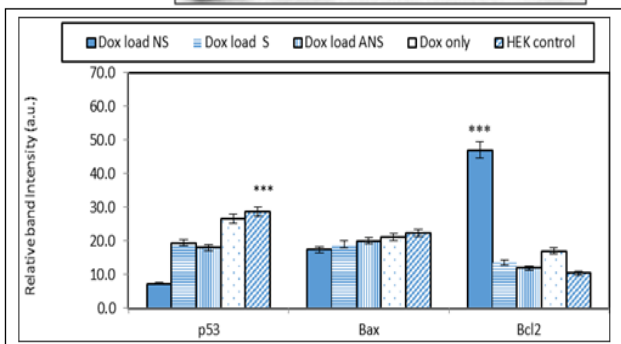
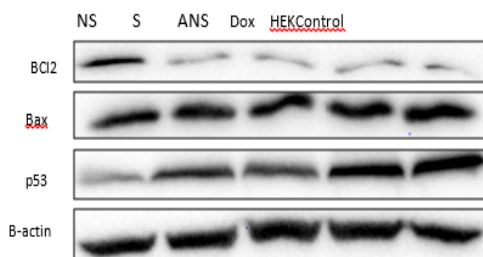


Figure 4: (a) Western blot analysis data of HEK-293 cells for p53, Bax, Bcl2 proteins after treatment with Dox loaded S, NS, ANS or Dox alone. Significantly higher level of Bcl2 was noticed in Dox load NS as compared to other treatments and control (**= $0.001 < p$). **(b)** Histogram band intensity in HEK-293 cells.

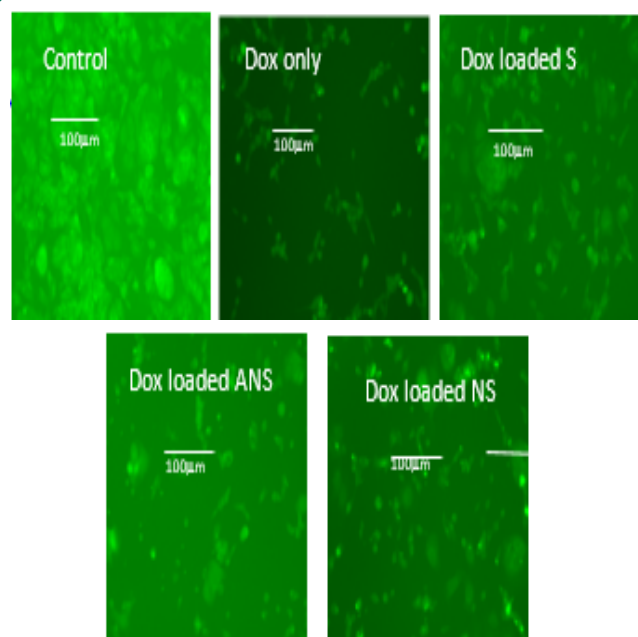


Figure 5: Fluorescence microscopic study for changes in mitochondrial membrane potential after staining with Rhodamine 123. Mitochondrial depolarization was observed in all treated cells. The Rhodamine123 fluorescence intensity, i.e. mitochondrial membrane potential decreased was observed more in Dox alone than in Dox loaded S, NS and ANS.

Doxorubicin loaded S, NS, ANS or Dox alone modulates p53, Bax and Bcl2: Intracellular ROS generation in apoptotic cells was associated with change in p53, Bax and Bcl2 protein expressions. Western blot analysis data (Fig. 4a) and band intensity histogram (Figure 4b) showed a significant increase in p53 and Bax protein expression, while slight decrease in Bcl2 expressions in Dox loaded S and ANS, but significant decreased in NS. In HEK cells, significant decrease was observed in Bcl2 expression, showing Dox loaded S, and ANS have similar anti-cancer effect like Dox alone. As expected, since HEK is not a cancer cell, higher concentration of Bax and p53 and lower Bcl2 were observed. Dox loaded NS showed less upregulation of Bax and

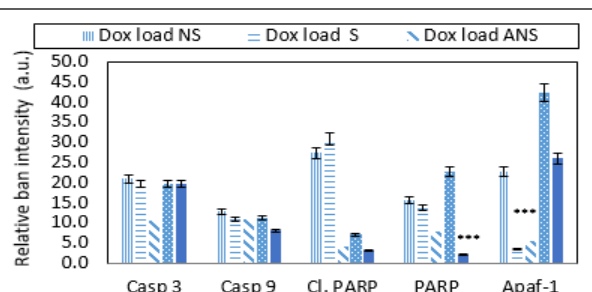
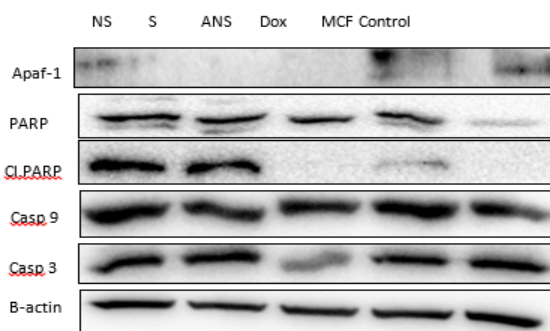


Figure 6: (a) Western blot analysis of mitochondrial signaling proteins in MCF7 cells. Activity of most of the proteins were up-regulated in Dox loaded S, NS or ANS or Dox alone. **(b)** Histogram represents up regulation of casp 9, cl. PARP and PARP.

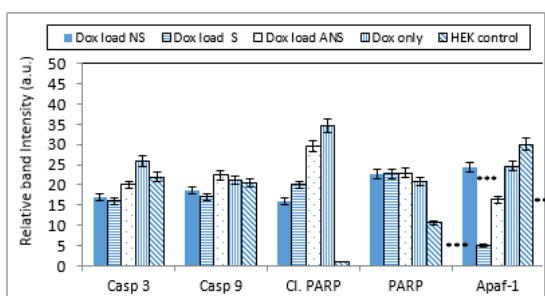
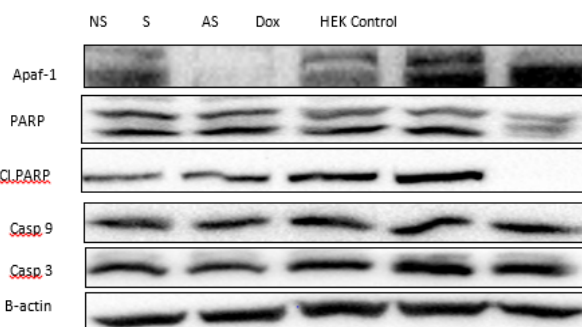


Figure 6: (a) Western blot of HEK cells treated with Dox loaded S, NS or ANS or Dox alone **(b)** Histogram of HEK cells with Dox loaded S, NS, ANS, or Dox alone. (**= $0.001 < P$).

p53 protein expression showing it caused less favorable signal transduction mechanism than Dox loaded S and ANS in normal cells (Figure 4a).

Doxorubicin loaded S, NS, ANS or alone depletes mitochondrial membrane potential: Generation of ROS in the cells by causing increased expression of p53 and Bax, and decreased Bcl2 are considered as indicators of activation of mitochondrial cell death pathway. The depletion of mitochondrial membrane potential of DOX loaded S, NS, ANS or DOX alone was demonstrated in Figure 5. This result clearly showed that the control MCF7 cells have higher fluorescence intensity than the treated cells. Interestingly, the depletion of the fluorescence intensity was significantly higher in cells treated with DOX alone than in cells treated with DOX loaded S, NS and ANS indicating that DOX

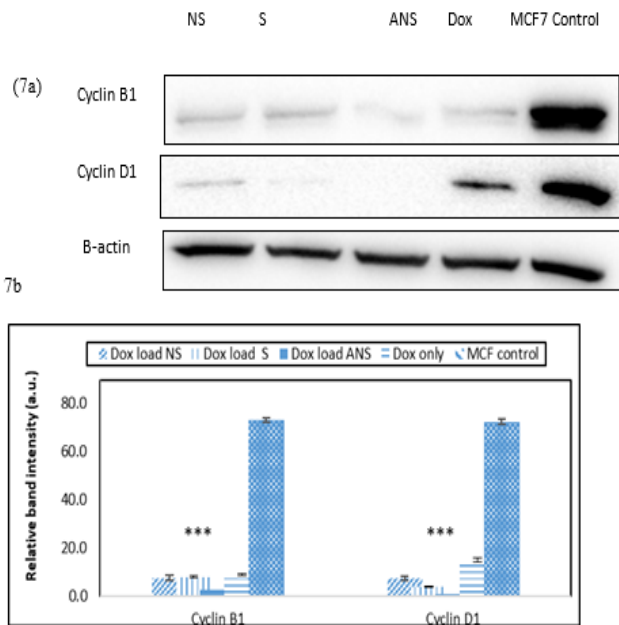


Figure 7: (a) Western blot analysis of cell cycle regulation protein Cyclin D1 and Cyclin B1. The expression of both proteins were down-regulated in Dox loaded SNS, ANS, or Dox alone as compared to control. **(b)** Histogram showed the significant decrease in cyclin D1 and B1 (** $p < 0.001$).

loaded S, NS and ANS were more effective in causing mitochondrial cell death than DOX alone.

Doxorubicin loaded S, NS, ANS or alone modulates mitochondrial signaling proteins: The depletion of mitochondrial membrane potential suggested the initiation of mitochondrial apoptosis pathway. Western blot analysis showed expression of casp 9, casp 3, cl. PARP, and PARP considered as very important event in cancer cell apoptosis (Figure 6a). The band intensity histogram showed increase of cl. PARP, PARP, and casp 9 expressions (Figure 6b). Slight increase in the expressions of casp 9, cl. PARP, and PARP were also observed in HEK-293 conveying the apoptotic effect of Dox loaded S, NS, and ANS on normal cells (Figure 6a and 6b).

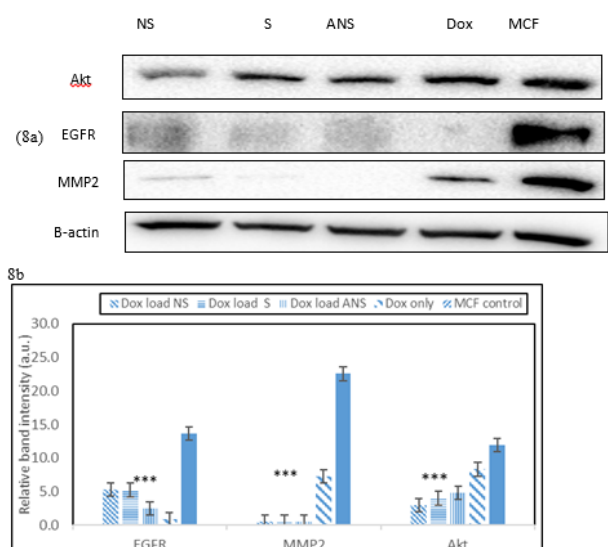


Figure 8: (a) Western blot analysis of expressions of Akt, EGFR and MMP2 in MCF7 cells treated with Dox loaded SNS, ANS, and Dox alone. The EGFR and MMP2 proteins were down-regulated in Dox loaded S, NS, ANS, or Dox alone showing the anti-invasive and anti-metastasis effect of Dox loaded in S, NS, or ANS. **(b)** Histogram showed significant decreased in these proteins (** $p < 0.001$).

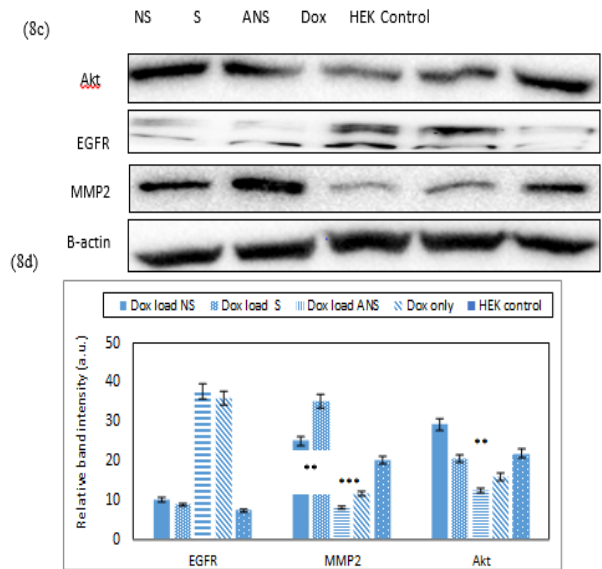


Figure 8: (c) Western blot of AKT, EGFR, and MMP2 in HEK-293 cells treated with Dox loaded S, NS, ANS, or Dox alone. **(d)** Histogram of Western blot from HEK-293. (** $p < 0.001$).

Doxorubicin loaded S, NS, ANS and alone modulates cell cycle regulatory proteins: Inhibition of cell cycle progression by causing apoptosis is also considered as one of the important strategies in the management of breast cancer. Western blot analysis data (Figure 7a) and the band intensity histogram (Figure 7b) showed that the expressions of both cyclin D1 and cyclin B1 were significantly decreased when cells were treated with Dox loaded S, NS, ANS or Dox alone than control MCF-7 cells.

Doxorubicin loaded S, NS, ANS and alone inhibit MMP2 and EGFR proteins: Inhibition of matrix metalloproteinase (MMP2) and epidermal growth factor (EGFR) are important strategies to decrease progression and metastasis of breast cancer cells. MMP2 degrades type 4 collagen, the most abundant component of the basement membrane. Degradation of the basement membrane is essential for metastatic progression and invasion of cancer cells property. Dox loaded S, NS, ANS significantly inhibit MMP2 better than Dox alone. Significant decrease in the protein's expression of EGFR and AKT were also observed in Dox loaded S, NS, ANS or Dox alone. Western blot analysis data of MCF-7 (Figure 8a) and the band intensity histogram (Figure 8b), and HEK and band intensity histogram (Figures 8c, 8d) are depicted.

Dox loaded S, NS, ANS and Dox alone induced cell death: Treatment of cells with Dox loaded S, NS, ANS and Dox alone caused similar cell death in comparison to control MCF7 cells. Dox alone caused less dead cells as compared to Dox loaded in NS or ANS, with significantly higher dead cells observed in DOX loaded S formulation. Figure 9a showed the expression of cells death/apoptotic (green) or cells alive (red or bright orange). Figure 9b showed histogram of apoptotic versus alive cells.

Discussion

MCF7 cells treated with Dox loaded NS, S, ANS or Dox alone exhibited important activation of apoptosis through nuclear condensation, increased in ROS generation, and collapse of membrane potential [16]. Hoechst33342 staining data suggested Dox loaded in S, NS, and ANS increased the nuclear condensation, which in turn increased the percentage of apoptotic cells. Generation of intracellular ROS plays a pivotal role in apoptosis. Evidences suggested that cancer cells generate more ROS than

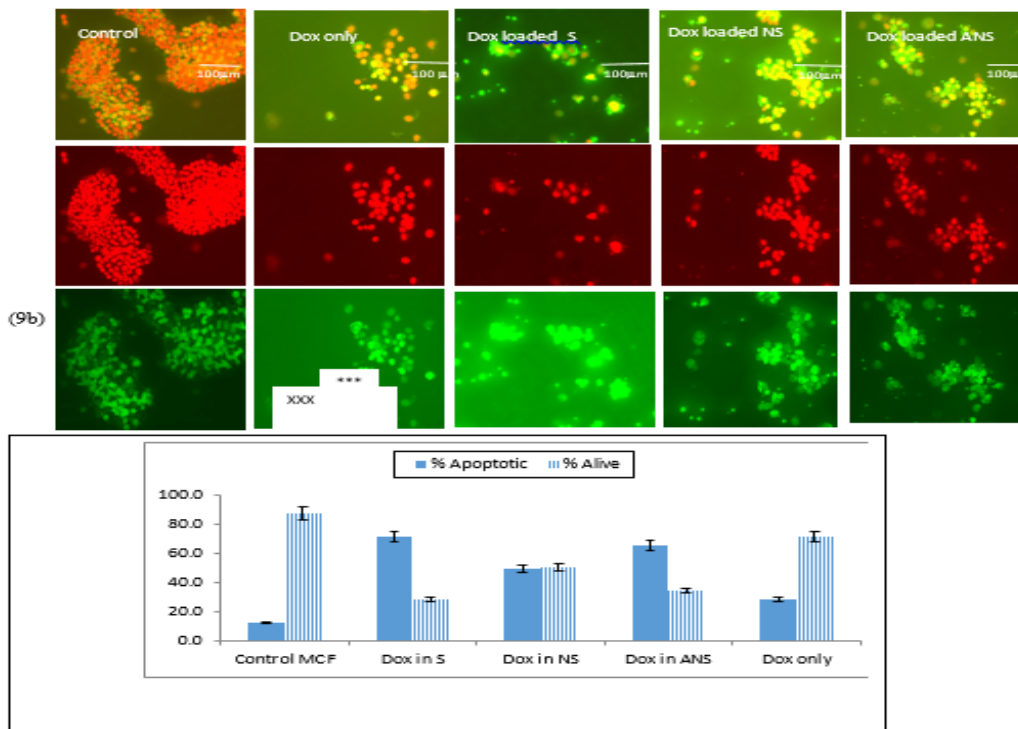


Figure 9: (a) Expression of cells death/apoptotic (green) or cells alive (red or bright orange). Scale bar indicated 100 μ m. **(b)** Histogram of apoptotic versus alive cells from different treatments. Dox loaded S, NS, ANS, or Dox alone caused significant increase in apoptotic cell versus control (**=0.01<p; ***=0.001<p).

normal cells which in turn caused cancer cells to apoptosis [17]. Increased ROS in cancer cells is associated with the activation of a key signaling protein p53. p53 plays important role in cell cycle regulation, DNA damage, cell apoptosis and tumor suppression [18,19]. ROS also plays crucial role in the modulation of pro-apoptotic Bax and anti-apoptotic Bcl2. Up regulation of p53 and Bax and down regulation of Bcl2 showed favorable signal transduction mechanism that triggers cancer cells to apoptosis in an orderly and sequential manner. Higher ratio of Bax/Bcl2 was noticed in Dox loaded NS followed by Dox alone, while Dox loaded S and ANS had similar Bax/Bcl2 ratio. Higher ratio of Bax/Bcl2 conveyed a more enhanced apoptotic efficacy. Mitochondria is one of the most important target organelle during the ROS mediated apoptosis in cancer cells. Intracellular ROS and subsequent Bax/Bcl2 modulation is proceeded by the collapse of mitochondrial membrane potential, which has been associated with the initiation of caspase cascade leading to cell death [20]. The present study showed that Dox loaded S, NS, or ANS showed depletion of mitochondrial potential, with Dox alone showed significant depletion of the potential.

Signaling proteins such as apaf-1 and cas 9 activate formation of apoptosome which further activates downstream executioner casp 3 protein. Casp 3 plays a central role in the execution of cancer cell apoptosis which is also responsible for the cleavage of PARP during cell death. Casp 3 and casp 9 are the major signaling proteins in inducing apoptotic cascade. Dox loaded NS, S or Dox alone caused DNA related damage in MCF7 cells by causing cleavage and higher expression of downstream protein PARP and cleaved PARP. Dox loaded ANS didn't cause activation of casp 3 nor cleaved or PARP.

Proliferation of cancer cells is also involved in altering regulation of cell cycle progression. The cell cycle progression is dependent on the activation of cyclin-dependent kinases (Cdk). The Cdk activation requires binding of a specific regulatory subunit cyclin. Among the cyclins, cyclinD1 and cyclinB1 plays fundamental role in the inhibition of breast cancer cell apop-

tosis [21-24]. Significant down regulation of cyclinD1 strongly suggested that Dox loaded S, NS or ANS were effective in inhibiting the G1-S cell cycle progression more than Dox alone. Furthermore, cyclinB1 down regulation in Dox loaded S, NS or S indicated the efficacy of these formulation in inhibiting G2 cell cycle progression.

Matrix metalloproteinase (MMPs) such as MMP2 plays important role in cancer invasion and metastasis by degrading extracellular matrix and basement component which play important role in microenvironment homeostasis. MMP2 not only control the extracellular matrix turnover and cancer cell migration, but it also regulates signaling pathways of cell growth, morphogenesis, angiogenesis, and tissue repair. MMP2 overexpression in cancer cells was related to poor prognosis [25,26]. Significant decrease in the MMP2 expression was observed in Dox loaded S, NS or ANS, with less decrease due to Dox alone.

Epidermal growth factor receptor (EGFR) overexpression in many solid cancers including breast cancer cause stimulation of downstream signaling pathways which induce cell growth, cell cycle progression, angiogenesis, cell motility and blocking of apoptosis cascade [27]. Significant decrease in the EGFR expression was observed in Dox loaded S, NS, ANS or Dox alone.

Activity of cytoprotective phosphatidylinositol-3 kinase (P13K)-Akt pathway often increased in cancer that could result from mutation, changed in proteins expression, or amplification of upstream growth-related factor [28]. Slight decrease in Akt expression was observed in Dox loaded S, NS, ANS, or Dox alone.

Conclusion

This study provides a novel approach for the delivery of Doxorubicin by loading starch nanocrystals with the drug. The doxorubicin-loaded starch nanocrystals were effective and can prevent side effects of cardiotoxicity when Doxorubicin is administered without the carrier.

Declarations

Authors' contributions: OAB: Conception, design, data collection, revision of manuscript, final approval of manuscript; LLB: Conception, design, experiments and data collection, draft of manuscript, revision of manuscript, final approval of manuscript. MAO: Extraction of starch, revision of manuscript, final approval of manuscript.

Conflicts of interest: The authors declare that they have no conflicts of interest.

Ethical approval: Not applicable.

Consent to participate: Not applicable.

Consent for publication: Not applicable.

Availability of data and materials: Not applicable.

Funding: The research was funded by Union University.

References

1. Block KI, Gyllenhaal C, Lowe L, Amedei A, Ruhul Amin ARM, Amin A, Aquilano K, Arbiser J, et al. Designing a broad-spectrum integrative approach for cancer prevention and treatment. *Seminars in Cancer Biology*. 2015; 35: 276-304. Doi: <https://doi.org/10.1016/j.semcancer.2015.09.007>.
2. Zhong Y, Meng F, Deng C, Mao X, Zhong Z. Targeted inhibition of human hematological cancers in vivo by doxorubicin encapsulated in smart lipoic-crosslinked hyaluronic acid nanoparticles. *Drug Delivery*. 2017; 24: 1482-90. DOI: 10.1080/10717544.2017.1384864.
3. Miles JS, Sojourner SJ, Whitmore AM, Freeny D, Darling-Reed S, Flores-Rosazs H. Synergistic effect of endogenous and exogenous aldehydes on doxorubicin toxicity in yeast. *BioMed Res Inter*. 2018; 4938189. Doi:10.1155/2018/4938189.
4. Andretta C, Minisini AM, Miscori M, Puglisi F. First-line chemotherapy with or without biologic agents for metastatic breast cancer. *Crit Rev Oncol/Hematol*. 2010; 76: 99-111. DOI: 10.1016/j.critrevonc.2010.01.007.
5. Shafei A, El-Bakly W, Sobhy A, Wagdy O, Reda A, Aboelenin O, et al. A review on the efficacy and toxicity of different doxorubicin nanoparticles for targeted therapy in metastatic breast cancer. *Biomed Pharmacother*. 2017; 95: 1209-18. DOI: 10.1016/j.biopha.2017.09.059.
6. Minotti G, Menna P, Salvatorelli E, Cairo G, Gianni L. Anthracyclines: molecular advances and pharmacology developments in antitumor activity and cardiotoxicity. *Pharmacol Rev*. 2004; 56: 185-29. DOI: 10.1124/pr.56.2.6.
7. McGowan JV, Chung R, Maulik A, Piotrowska I, Walker JM, Yellom DM. Anthracycline chemotherapy and cardiotoxicity. *Cardiovasc Drugs Ther*. 2017; 31(1): 63-75. doi: 10.1007/s10557-016-6711-0.
8. Turner N, Biganzoli L, DiLeo A. Continued value of adjuvant as treatment for early breast cancer. *The Lancet Oncol*. 2015; 16: 362-69.
9. Omoteso OA, Adebisi AO, Kaiyaly W, Asare-Addo K, Odeniyi MA. Effect of pregelatinization and carboxymethylation on starches from African rice and Fonio: Influence on release of low melting-point drug. *British J Pharm*. 2020; 4(2): 1-15. doi: <https://doi.org/10.5920/bjpharm.645>.
10. Mao SR, Chen ZM, Wei ZP, Liu H, Bi D. Intranasal administration of melatonin starch microspheres. *Int J Phytorem*. 2004; 272(1-2): 37-43. DOI: 10.1016/j.ijpharm.2003.11.02.
11. Xiao H, Yang T, Lin H, Liu G, Zhang L, Yu F, Chen Y. Acetylated starch nanocrystals: preparation and antitumor drug delivery study. *Int J Biol Macromol*. 2016; 89:456-64. doi: 10.1016/j.ijbiomac.2016.04.037.
12. Lawal MV, Odeniyi MA, Itiola OA. Material and rheological properties of native, acetylated and pregelatinised forms of Corn, Cassava and Sweet Potato starches. *Starch/Starke*. 2015; 67(11-12): 964-75. <https://doi.org/10.1002/star.201500044>.
13. Bamiro OA, Odeniyi MA, Addo RT. Native and modified Oryza glaberrima Steud starch nanocrystals: Solid-state characterization and anti-tumour drug release studies. *British J Pharm*. 2021; 6(1): 790. <http://doi.org/10.5920/bjpharm.790>.
14. Mondal A, Bennett L. Resveratrol enhances the efficacy of sorafenib mediated apoptosis in human breast cancer MCF7 cells through ROS, cell cycle inhibition, caspase 3 and PARP cleavage. *Biomed Pharmacother*. 2016; 84: 1906-14. DOI: 10.1016/j.biopha.2016.10.096.
15. Bennett LL, Mondal A. Curcumin and afatinib synergistically inhibit growth of human osteosarcoma cells by inhibition of matrix metallo proteinases, mitogen activated kinases 1-4, and reactive oxygen species. *J of Pharmacy and Drug Dev*. 2021; 3(1).
16. Hengartner MO. The biochemistry of apoptosis. *Nature*. 2000; 407: 770-76. doi:10.1038/35037710.
17. Simon HU, Haj-Yehia A, Levi-Schaffer F. Role of reactive oxygen species (ROS) in apoptosis induction. *Apoptosis*. 2000; 5: 415-18. doi:10.1023/A:1009616228304.
18. Mates JM, Sanchez-Jimenez FM. Role of reactive oxygen species in apoptosis: implications for cancer therapy. *Int. J. Biochem. Cell Biol*. 2000; 32:157-70. doi:10.1016/S1357-2725(99)00088-6.
19. Zhang T, Brazhnik P, Tyson JJ. Exploring mechanisms of the DNA-damage response: p53 pulses and their possible relevance to apoptosis. *Cell Cycle*. 2007; 6: 85-94. doi:10.4161/cc.6.1.3705.
20. Penninger JM, Kroemer G. Mitochondria, AIF and caspases-rivaling for cell death, *Nat Cell Biol*. 2003; 5: 97-9. doi:10.1038/ncb0203-97.
21. Aarts M, Linardopoulos S, Turne NC. Tumour selective targeting of cell cycle kinases for cancer treatment. *Curr. Opin. Pharmacol*. 2013; 13: 529-35. doi: 10.1016/j.coph.2013.03.012.
22. Roy PG, Thompson AM. Cyclin D1 and breast cancer. *Breast*. 2006; 15: 718-27. doi: 10.1016/j.breast.2006.02.005.
23. Suzuki T, Urano T, Miki Y, Moriya T, Akahira JI, Ishida T, et al. Nuclear cyclin B1 in human breast carcinoma as a potent prognostic factor. *Cancer Sci*. 2007; 98: 644-51. doi:10.1111/j.1349-7006.2007.00444.x.
24. Jiang WG, Sanders AG, Katoh M, Ungefroren H, Gieseler F, Prince M, et al. Tissue invasion and metastasis: Molecular, biological and clinical perspectives, *Semin cancer biol*. 2015; 35: 244-75. Doi: 10.1016/j.semcancer.2015.03.008.
25. Zhu XM, Sun WF. Association between between matrix metalloproteinases polymorphisms and ovarian cancer risk: A meta-analysis and systemic review. *PlosOne*. 2017. doi.org/10.1371/journal.pone.0185456.
26. Peng H, Liu L, Zhao X. Prognostic significance of matrix metalloproteinase-2 in gynecological cancer: a systemic review of the literature and meta-analysis. *JBUON*. 2013; 18: 202-10.
27. Maennling AE, Tur MK, Niebert M, Klockenbring T, Zeppernick F, Gattenlohner F, et al. Molecular targeting therapy against EGFR family in breast cancer: progress and future potentials. *Cancers*

(basel). 2019; 11 (12): 1826. DOI: 10.3390/cancers11121826.

28. Gallayas F, Sumegi B, Szabo C. Role of Akt activation in PARP inhibitor resistance in cancer. *Cancers (Basel)*. 2020; 12 (3): doi: 10.3390/cancers12030532.